analytical chemistry

Review

pubs.acs.org/ac

Nanoscale Electrochemistry

Stephen M. Oja, Marissa Wood, and Bo Zhang

Department of Chemistry, University of Washington, Seattle, Washington 98195, United States

CONTENTS

This Review reports recent advances in the field of nanoscale electrochemistry. We specifically focus on new electrochemical phenomena, properties, and technological capabilities essential to reducing the dimensions of an electrochemical probe to the nanometer scale, as well as electrochemical properties of new nanoscale electrode materials. Here, we adopt the conventional definition of nanoscale to refer to lengths between 1 and 100 nm. Nanoscale electrochemistry is critically important for modern electrochemical science as well as many other key research areas, such as energy conversion and storage, catalysis, sensor development, and environmental science. Nanoscale electrochemical investigations have provided unique information unattainable using traditional methods. For example, nanoelectrodes can measure ultrafast electron-transfer kinetics that are often too fast to investigate with conventional electrodes. Nanoscale electrochemical materials, such as metal/semiconductor nanoparticles, have unique chemical and physical properties, and nanoscale electrochemical methods can be used to prepare advanced electrocatalytic materials. In addition, the use of nanoscale electrode probes has enabled electrochemical imaging with nanoscale spatial resolution, yielding unique information for better understanding heterogeneous electrode/solution interfaces.

Nanoscale electrochemistry is a rather broad topic, as electrochemistry deals with electron- and charge-transfer processes at solid/liquid and liquid/liquid interfaces. These processes are inherently nanoscale by nature. Here, we restrict the scope of this Review and choose to focus on the following aspects: (1) preparation, characterization, and use of nanometer scale electrochemical probes including nanoelectrodes and nanopores; (2) theory and experiments for better understanding electron and mass transfer at nanoelectrodes; (3) faradaic processes of nanoscale redox species, e.g., metal nanoparticles and single redox molecules; (4) electrochemical techniques to prepare nanomaterials; (5) electrochemical imaging to achieve nanoscale spatial resolution. The field of nanoscale electrochemistry began about three decades ago shortly after the fast development and widespread application of microelectrodes. Since then, this field has generated enormous excitement and has seen a dramatic increase in popularity in the last two decades. This growth is largely due to rapid developments in nanofabrication and characterization and the introduction of numerous bottom-up and top-down processes capable of preparing well-defined nanoelectrodes and materials.

NANOELECTRODES

The early development and use of very small electrodes, i.e., electrodes below 10 μm, was largely driven by the need to detect and monitor the fast release kinetics of electroactive neurotransmitter molecules in the brain.[1] In the early 80s, Wightman[2,3] and others[4,5] reported the construction and use of ultramicroelectrodes (UMEs) in electrochemical measurements.

Special Issue: Fundamental and Applied Reviews in Analytical Chemistry 2013

Published: November 2, 2012

   dx.doi.org/10.1021/ac3031702 | *Anal. Chem.* 2013, 85, 473−486

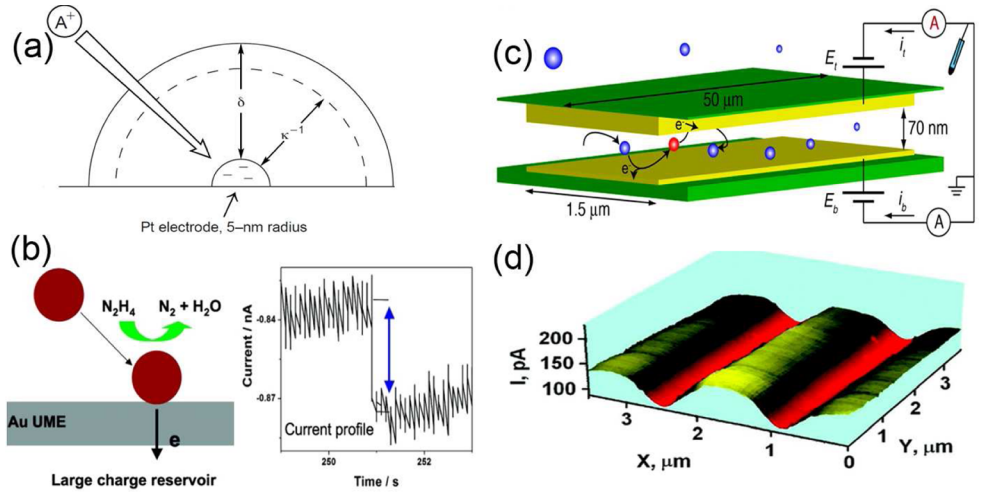

Figure 1. (a) A schematic diagram of a 5 nm radius nanoelectrode in a 0.2 mM 1:1 electrolyte, its diffusion layer thickness, δ, and the electrical double layer thickness, κ^{-1}. A cation redox molecule is attracted to the electrode, resulting in an enhanced transport rate. Reprinted from ref 70. Copyright 2005 American Chemical Society. (b) Principle of Bard's single nanoparticle collision experiments: (left) diagram of single NP collision at a Au UME surface; the reaction is switched on when the particle is in contact with the detection electrode; (right) representative current profile observed in a single NP collision event. Reprinted from ref 109. Copyright 2008 American Chemical Society. (c) Principle of Lemay's single-molecule electrochemistry device. Redox-active molecules undergoing Brownian motion are repeatedly oxidized and reduced at two parallel electrodes causing a measurable current. Reprinted from ref 133. Copyright 2011 American Chemical Society. (d) Constant-height SECM image of a 3.5 μm × 3.5 μm portion of a CD surface obtained with a 190 nm Pt tip in ionic liquid containing 50 mM Fc. Reprinted from ref 225. Copyright 2009 American Chemical Society.

In one of his early reviews, Wightman described the major advantages of the use of UMEs for electrochemical measurements, which include small R_sC_{dl} time constants, miniaturized electrode dimensions, and very small iR_s drop due to extremely small currents, where i is the current, R_s is the solution resistance, and C_{dl} is the double layer capacitance. These extraordinary properties are apparently more predominant for electrodes with smaller dimensions, e.g., nanoelectrodes. In fact, Wightman pointed out some possible advantages of the use of electrodes as small as 10 nm. Nanoelectrodes were first used in electrochemical experiments in the mid-1980s. Band shape nanoelectrodes were developed and reported by several groups including Wightman,[6] Bond,[7] and White.[8] This field has since seen rapid growth, owing to the use of nanoelectrodes of various sizes and geometries.

Extraordinary Properties of Nanoelectrodes. Nanoelectrodes are generally defined as electrodes possessing at least one dimension less than 100 nm. As with other nanoscale structures, nanoelectrodes display significantly different behavior than their macroscopic counterparts. As one might expect, these deviations in electrochemical behavior have been exploited by researchers to investigate new areas of both fundamental and applied electrochemistry. Perhaps the most obvious benefit of shrinking the working electrode is the ability to do electrochemistry in increasingly small spaces. These small spaces include single biological cells[9−11] and what may be the ultimate goal of scaling down the working electrode, single-molecule electrochemistry.[12,13] Shrinking the working electrode to the nanoscale has also given rise to widely used techniques such as scanning electrochemical microscopy (SECM)[14] and its variants (i.e., SECM-atomic force microscopy (AFM)[15,16]).

An intrinsic electrochemical benefit of a smaller electrode is the decrease of the electrical double layer capacitance, C_{dl}, which decreases as electrode area decreases. This results in a dramatically decreased time constant, R_sC_{dl}, allowing experiments to be done on nanosecond time scales.[17,18] Wightman first demonstrated the use of carbon UMEs to run cyclic voltammetry experiments at 10^5 V/s.[19,20] Amatore[21,22] and others[23,24] have reported the use of scan rates up to 10^6 V/s with specially designed potentiostats and UMEs. With such small electrodes, electrochemical measurements can be carried out in the nanosecond time domain, enabling the direct study of ultrafast electrochemical kinetics and detection of short-lived intermediate species. Another result of decreased electrode size is the ability to do experiments in media with a very large electrical resistance, such as a solution without the addition of a supporting electrolyte.[25] Thus, nanoelectrodes enable electrochemical experiments to be carried out at time scales and in media unfeasible using larger electrodes.

Another significant effect of scaling down electrode size is that radial diffusion is the dominant form of mass transport to the nanoelectrode surface. This results in faster mass transport than for larger electrodes, which allows the study of very fast electron-transfer kinetics via steady-state experiments.[26,27] Lastly, nanoelectrodes enable the investigation of many interesting fundamental processes and phenomena in electrochemistry. Figure 1a illustrates a comparison of electrode size, diffusion layer thickness, and electrical double layer thickness for a 5 nm radius hemispherical nanoelectrode in a 0.2 mM 1:1 electrolyte solution. What happens when the size of the electrode, diffusion layer, double layer, and molecule are all comparable? This question presents the complicated electrochemistry that can be explored with nanoelectrodes. Murray's 2008 review[28] of nanoelectrochemistry pointed out several possible fundamental issues that could be researched using nanoelectrodes. These include the study of double layer structure, mass transport within a diffusion layer of comparable size to the double layer, reactions of molecules on electrode interfaces of comparable size, and quantum size effects of small nanoelectrodes.

Nanoelectrode Fabrication. The first nanoelectrode used in voltammetric studies was the nanoband electrode, made by depositing a thin-film of electrode material onto a glass slide, insulating the thin-film, and then polishing the edge of the slide

dx.doi.org/10.1021/ac3031702 | Anal. Chem. 2013, 85, 473−486

to expose the electrode.[6] The thickness of the thin metal film therefore determined the critical dimension of the electrode. Since then, nanoelectrodes possessing a variety of geometries have been fabricated, including nanodisks, -rings, -hemispheres, -cylinders, and most recently, -pores. With such extensive research into nanoelectrode fabrication, it is no surprise that many methods have been developed for the fabrication of each type of electrode geometry. Zoski,[29] Arrigan,[30] and most recently Cox and Zhang[31] have reviewed the different nanoelectrode geometries and the fabrication methods used to achieve those geometries. Common fabrication methods include: laser-assisted micropipet pulling;[32−34] insulation and subsequent exposure of an electrochemically sharpened metal wire or carbon fiber (insulator = glass,[35−37] electrophoretic paint,[26,38,39] polyimide,[40] Teflon,[41] wax[42]), deposition of thin-films onto planar or cylindrical substrates, followed by insulation and exposure of the metal to produce nanoband[43,44] and nanoring[45−48] electrodes, respectively; and electrochemical etching of nanodisk electrodes to form nanopore electrodes.[49−51] Readers are referred to the reviews of Zoski,[29] Arrigan,[30] and Cox and Zhang[31] for details on the methods and materials previously used to make nanoelectrodes.

Despite the vast number of fabrication methods reported, most follow the same general procedure used by Wightman to fabricate the first useful nanoelectrode. This approach consists of encapsulating or sealing the electrode material in an insulator and then either mechanically polishing or chemically etching away the insulator to expose the electrode. A major advantage of this technique is that it is typically cheap and requires little specialized equipment (i.e., photolithography equipment, cleanroom, etc.). These two features make nanoelectrode fabrication achievable for many different researchers, with little need for advanced training or in-depth knowledge of technical processes.

However, the "seal and polish/etch" technique is not without problems, namely, lack of reproducibility and lack of nanoscale control over the electrode dimensions. While methods like polishing and micropipet pulling offer some control (i.e., polishing material and time and programmable pulling parameters, respectively), there is still limited ability to control the dimensions at the nanometer-scale. This lack of dimensional control is directly related to the lack of reproducibility, making it difficult to consistently fabricate identical nanoelectrodes. "Leakage," caused by a poor seal between the electrode and insulator, is also a persistent problem that renders many nanoelectrodes unusable.

An issue with all nanoelectrodes, regardless of the method of fabrication, is proper electrochemical characterization. Not only must the size of the electrode be known (i.e., radius of a nanodisk), but also the geometry of both the electrode and the surrounding insulator, as all three factors affect mass transport. Limiting current measurements are commonly used to estimate the size of a nanoelectrode. However, this requires an assumption about both the electrode geometry and the geometry of the surrounding insulator. For a disk electrode, $i_{ss} = 4nFDC^*r$,[52] where i_{ss} is the diffusion-limited steady-state current, n is the number of electrons transferred, F is Faraday's constant, D and C^* are the diffusion coefficient and bulk concentration of the redox species, respectively, and r is the radius of the electrode. This equation assumes that the exposed electrode surface is a perfect circle and is in the same plane as the surrounding insulator. However, if the electrode is recessed into the insulator, some radial lines of diffusion become blocked, and the limiting current is underestimated. This results in an underestimation of electrode size. Conversely, if the electrode protrudes from the surrounding insulator, additional lines of radial diffusion are exposed, leading to an overestimation of electrode size. Deviations in the electrode geometry from the assumed geometry lead to similar over/underestimations of electrode size. Therefore, electrochemical characterization via a limiting current method requires microscopic verification of both electrode size and geometry, as well as the geometry of the surrounding insulator.

Although SECM has been developed to address this problem, it highlights another issue of the seal and polish/etch technique, which is the fact that it is a serial production method. Because only one electrode (or array of electrodes) is fabricated at a time, and the fabrication method is not reproducible, each electrode requires individual microscopic imaging for full and accurate electrochemical characterization. A method in which several identical nanoelectrodes could be made simultaneously would be beneficial from the standpoint of both reproducibility and minimization of time spent imaging. Assuming identical electrodes, imaging one electrode would be the same as imaging the entire batch of electrodes. This Review will now highlight several newer nanoelectrode fabrication techniques that do not follow the traditional "seal and polish/etch" technique.

Nanoskiving. Nanoskiving is a technique of particular interest due to the versatility it affords despite being relatively cheap and simple. Developed by the Whitesides group as an alternative to conventional top-down nanofabrication techniques, nanoskiving can be used to fabricate nanoelectrodes (as well as a myriad of other nanostructures), either singly or in an array, with control over all three dimensions.[53−55] The nanoskiving procedure consists of three general steps: (1) deposition of a film of the desired electrode material onto an epoxy substrate, (2) embedding the film in epoxy to create an epoxy block, and (3) sectioning the epoxy block into slabs using an ultramicrotome. The three dimensions of the structure are thus defined by (1) the thickness of the deposited film, (2) the topography of the surface onto which the film is deposited (the epoxy substrate can be patterned via soft lithography), and (3) the thickness of the slabs cut by the ultramicrotome.

In the first report of nanoskiving, Xu et al. fabricated an array of Au nanoband electrodes with a critical dimension of 50 nm.[56] In a later report from the Whitesides group, Dickey et al. fabricated individually addressable parallel nanowire electrodes with a spacing of only 30 nm.[57] Recently, Dawson et al. reported the use of nanoskiving to fabricate a single Au nanowire electrode device.[58] These three reports highlight the range of controlled-dimension nanoelectrodes that can be produced using nanoskiving, all without the need for state-of-the-art lithographic equipment and clean rooms that are unavailable in many academic laboratories. In addition to providing control over all three electrode dimensions, nanoskiving is also exciting in that it can produce many identical electrodes at a time, thus eliminating the need to image each individual electrode.

Lithographically Patterned Nanowire Electrodeposition. Developed by Penner and co-workers, lithographically patterned nanowire electrodeposition (LPNE) is a technique that combines top-down photolithographic methods with bottom-up electrochemical synthesis to fabricate both individual nanowires and nanowire arrays. In the first publication of this "best of both worlds" technique, Menke et al. reported the fabrication of rectangular nanowires with heights down to 18 nm and widths down to 40 nm, providing independent control over both parameters with approximately 5 nm precision.[59] The process consists of the use of photolithography to create a

dx.doi.org/10.1021/ac3031702 | Anal. Chem. 2013, 85, 473−486

sacrificial nickel nanoband electrode that is recessed in a horizontal trench. The nanowire is then created via electrodeposition of a metal at this recessed nanoband electrode. It is the trench that defines the height of the nanowire, while the duration of electrodeposition controls the width. Removal of the photoresist and sacrificial nickel electrode results in an exposed nanowire. LPNE has subsequently been used to produce nanowire arrays of many different types of materials, including gold, silver, platinum, palladium, CdSe, PbTe, and PbSe.[60−63]

A fundamental limitation of nanowire arrays created via LPNE is the separation between the nanowires. This distance is defined by photolithography and is therefore limited to approximately half the wavelength of the photolithography light source. To overcome this limitation and produce high-pitch arrays of nanowires, Menke and co-workers have developed a variation of LPNE termed high-density lithographically patterned nanowire electrodeposition (HD-LPNE).[64] In this method, after the nanowire material is electrodeposited onto the sacrificial nickel electrode, nickel is deposited onto the nanowire material. This process of alternating electrodeposition is repeated, creating nanowires sandwiched between nickel. After removing the photoresist and nickel, an array of nanowires remains. The size and composition of the nanowires is determined by the deposition parameters of the nanowire material, while the spacing between nanowires is determined by the deposition parameters of the nickel. Using this technique, they reported an array of parallel 50 nm gold nanowires with separations as small as 50 nm.

SWNT-Templated Nanowires and MCEM. Unwin and co-workers recently reported the fabrication of submillimeter long metal nanowires with sub-100 nm heights via a single-walled carbon nanotube (SWNT) template method.[65] Metal is electrodeposited onto flow-aligned SWNTs, allowing control over the nanowire height down to 30−40 nm based on electrodeposition time. This technique is unique among current nanoelectrode fabrication methods in that it requires no photolithography, etching, encapsulation/sealing, or polishing but can give electrodes of controllable dimensions and geometry. Voltammetric analysis was performed on both the metal nanowires and pure SWNTs using the microcapillary electrochemical method (MCEM). In this method, a capillary with an inner diameter of 30−70 μm is filled with a solution containing a redox-active species. A reference electrode is placed in the capillary solution, and the capillary is placed above the nanowire so that the solution meniscus covers the wire, thus completing an electrochemical cell. Using MCEM, the solution is automatically confined to a defined area, eliminating the need to electrochemically isolate the rest of the nanowire from the solution. Additionally, multiple measurements can be made on the same sample by simply moving the microcapillary to a new location.

VOLTAMMETRY AND DOUBLE LAYER EFFECTS ON NANOELECTRODES

The unique size-dependent electrochemical properties of UMEs and nanoelectrodes have attracted enormous research interest in the last three decades. Delmastro and Smith first solved the voltammetry of spherical UMEs followed by more recent work by Bond and Oldham.[66,67] Saito first described the analytical equation for the steady-state limiting current at a disk-shape microelectrode.[68] The Butler−Volmer formalism[52] has traditionally been considered when describing the electrochemical response of UMEs and nanoelectrodes. Oldham and Zoski reported an empirical expression for the steady-state current−voltage response at an inlaid disk UME for reversible, quasi-reversible, and irreversible reactions.[69] Previous derivations of the current−voltage response of disk-shape UMEs often involve solving Fick's diffusion equations in conjunction with the Butler−Volmer formalism.

The electrochemical behavior of nanoelectrodes can be significantly more complicated than that of UMEs. A number of key factors may greatly alter their voltammetric behavior. These include the possible overlap of the electrical double layer and the diffusion layer,[70] edge effects,[71] the inaccuracy in describing the exact size and geometry of the electrodes,[72] and more importantly, the validity of the Butler−Volmer equations.[73] In a recent report,[73] Feldberg pointed out that the Butler−Volmer model may not be the correct model to describe the electrochemical response of nanoelectrodes due to their fast mass-transfer kinetics. The Butler−Volmer model assumes that the heterogeneous electron-transfer rate constant increases exponentially with potential $(E - E^{o\prime})$ without a limit. Using the Marcus−Hush formalism,[74−76] Feldberg analyzed the steady-state voltammetric response of a nanoelectrode and showed that both the limiting current and the shape of the CV response are likely strongly affected by the electron-transfer kinetic limitation. In fact, when the electrode size is sufficiently small, the electron-transfer rate may not be able to keep up with the mass-transfer limited current yielding a steady-state limiting current smaller than the diffusion-limited current. The Marcus−Hush formalism has also been used by Chidsey in analyzing electron-transfer rate constants across organic monolayers.[77]

Effect of Electrical Double Layer. Electrochemists have long considered the effects of supporting electrolyte on the voltammetric response of UMEs[78−80] and nanoelectrodes.[81] These effects are mainly due to electrostatics and can be ascribed to the promotion or inhibition of redox flux from migration. Amatore and co-workers have developed a series of useful equations to describe the change in limiting current at UMEs in the absence of a supporting electrolyte.[78,79] The validity of these predictions has been confirmed with electrodes as small as 1 μm or below.[82] However, it is important to note that, when nanoelectrodes are used, additional changes to the limiting current are often observed which are difficult to explain by migration alone.

Several lengths must be considered when discussing the effects of the electrical double layer. These include the critical dimension of the nanoelectrode, the thickness of the diffusion layer, and the thickness of the electrical double layer. For a spherical nanoelectrode, the diffusion layer thickness can be approximated as 10 times the radius of the electrode.[52] The electrical double layer has a characteristic thickness of the Debye length, κ^{-1}. The thicknesses of the electrical double layer and the diffusion layer in Figure 1a are drawn to scale for an easy comparison of their relative length. A cation redox species, e.g., $Ru(NH_3)_6^{3+}$, approaching the electrode surface will experience electrostatic attraction which will enhance the rate of mass transport resulting in an increased limiting current. This electrostatic enhancement effect is greatly reduced in a highly concentrated electrolyte solution, e.g., 3 M KCl. In this case, the double layer thickness is decreased down to a few Å, which is significantly smaller than the thickness of the diffusion layer.

White and co-workers were among the first to consider the electrical double layer effect on the diffusion-limited steady-state current of nanoelectrodes.[43,83,84] They suggested that the electrostatic effect must be considered when the electrode size is comparable to the Debye length. They used a parameter $r_o\kappa$ in their discussion, showing that, when $r_o\kappa$ is less than 100, the double layer effect becomes significant. Conyers and White reported the use of Pt nanoelectrodes in the range of ~2 to 2000 nm

dx.doi.org/10.1021/ac3031702 | Anal. Chem. 2013, 85, 473−486

to study the effect of supporting electrolyte.[85] They have shown that, when the electrode is below 10 nm, the limiting current for the oxidation of a positively charged redox species, ferrocenylmethyltrimethylammonium ($FcTMA^+$), is less affected by the absence of supporting electrolyte. They attributed this observation to a strong double layer effect when the electrode size becomes comparable to the Debye length. Similar effects have been found with other redox species, such as ferrocene, 1,1′-ferrocenedimethanol, and negatively charged ferrocene monocarboxylate ($FcCOO^-$).[86] Chen and Kucernak have investigated this interesting phenomenon using carbon nanoelectrodes approaching 1 nm and also found strong deviations from Amatore's predictions when electrodes are below a certain size.[87] In another study, Chen and Kucernak observed even stronger effects on the limiting current using several redox species with different charges: $Fe(CN)_6^{3-}$, $Fe(CN)_6^{4-}$, $Ru(NH_3)_6^{3+}$, and $Ir(Cl)_6^{2-}$. Interestingly, these redox species all show strong inhibition of the limiting current in the absence of supporting electrolyte.[88]

What causes the strong enhancement or inhibition of the limiting current in the absence of excess supporting electrolyte remains unclear. However, there are several possible contributions. First, the lack of excess supporting electrolyte may cause a significant decrease of the electron-transfer rate constant, an effect first proposed by Frumkin.[52] This decrease is due to a smaller potential drop at the electrode/solution interface in the absence of a compact double layer. Frumkin also considered a possible change to the effective concentration at the electrode/solution interface caused by the lack of excess supporting electrolyte. Chen and Kucernak also suggested that the dynamic nature of the diffuse double layer could be partially responsible for the observed deviation from the Amatore prediction for very small nanoelectrodes.[88] Such dynamic properties have previously been considered by White and co-workers when modeling double layer effects on nanoelectrodes.[80,89]

The results of Chen and Kucernak using carbon nanoelectrodes not only clearly show the strong double layer effect on the steady-state limiting current but also further prove that there is also a strong effect on electron-transfer kinetics.[88] Interestingly, different redox species were found to respond quite differently to changes in the electrolyte concentration. For example, the apparent electron-transfer rate constant of $Fe(CN)_6^{3-}$ decreases very quickly in the absence of supporting electrolyte. On the other hand, $Ru(NH_3)_6^{3+}$ is less sensitive to the change in the supporting electrolyte concentration. Watkins and White carried out another study using Pt nanoelectrodes and $FcTMA^+$ and $Ir(Cl)_6^{3-}$ as redox species.[90] Their results revealed that the electron-transfer rate for the oxidation of $Ir(Cl)_6^{3-}$ increases quite dramatically in the presence of a supporting electrolyte. Interestingly, they also found that the half-wave potential for the oxidation of $Ir(Cl)_6^{3-}$ shifts to more positive potentials in the presence of a supporting electrolyte. They suggested that there is a clear ion-pairing effect responsible for the cation-dependent potential shift. A similar but stronger effect has recently been predicted by Chen and co-workers.[91]

Chen and co-workers have done some elegant work investigating the size- and double layer-dependent voltammetric response of nanoelectrodes.[92−94] They modeled steady-state voltammetric behaviors of nanoelectrodes by considering the dynamic nature of the electrical double layer during the potential ramping.[95] They found that both the shape of voltammogram and its limiting current could be affected by several factors such as the charge of the redox species, the size of the electrode, and the dielectric properties of the electrical double layer. In a recent publication,[94] they modeled the size-dependent voltammetric response of nanoelectrodes using three different theories: the Butler−Volmer theory, the Marcus theory, and Chidsey's model.[77] Their results also predict that the electron-transfer rate constant, k^o, could vary and that the Butler−Volmer theory might be invalid when the electrode is below 10 nm.

NANOPARTICLE ELECTROCHEMISTRY

Nanoparticles are of great interest to chemists for a number of reasons, particularly as catalysts. Their high surface-to-volume ratio and size-dependent electronic properties make them an intriguing and useful entity to study. It has been found that nanoparticles of different sizes and structures can show significantly different catalytic activities.[96,97] Therefore, understanding the structure−function relationship of nanoparticles is crucial to understanding their catalytic properties.[98] In typical electrocatalytic studies, nanoparticles are studied as ensembles, with many nanoparticles immobilized on an electrode.[99−101] Hence, the electrocatalytic information gained from such a study is the result of the average properties of the ensemble. Valuable information has been gained using ensemble-based methods, including the effect of nanoparticle size[102] and composition[103] on electrocatalytic activity. However, gaining a true fundamental understanding of nanoparticle structure−function relationships as they relate to electrocatalysis requires performing electrochemistry on individual nanoparticles. Much research has been done recently to develop methods for single nanoparticle electrochemistry, and they will be reviewed here.

Monolayer Protected Clusters. Monolayer protected clusters (MPCs) specifically refer to nanoparticles consisting of a small Au core stabilized by an organothiolate ligand monolayer.[104] The Au cores typically range in average size from 1 to 5 nm.[105] The extensive research done on MPCs over the past 20 plus years has been enabled by the fact that they are isolable, enabling them to be repeatedly isolated from and redissolved in solution without aggregation or decomposition. The synthesis of MPCs is done using the Brust synthesis, first reported by the Schiffrin lab.[106] Since this initial report, substantial research effort has been put into both directly altering aspects of the synthesis and postreaction modification of the products to produce MPCs with different properties (i.e., size, solubility, voltammetric response, etc.).[107] Many electrochemical studies have been done on both solutions of MPCs and films of MPCs coated on electrodes. At this point, we refer readers to two excellent reviews for more information on MPCs. The review by Templeton et al.[104] provides an overview of many fundamental characteristics of MPCs as well as a summary of early experimental work (both synthetic and electrochemical) on MPCs. Murray's review,[105] written 8 years later, provides a very thorough summary of MPCs, highlighting the many interesting electrochemical studies that have been done on a wide range of MPCs.

Stochastic Nanoparticle Electrochemistry. Developed by the Bard group, this is an elegant experimental approach used to study single nanoparticles by monitoring single nanoparticle collisions with an UME.[108,109] As illustrated in Figure 1b, this approach is based on electrocatalytic amplification, wherein an UME is held at a constant potential at which it is kinetically inert toward a redox reaction of interest. When a nanoparticle that displays electrocatalytic activity toward the reaction of interest collides with the electrode, it catalyzes the reaction and results in a large current increase. This increase in current is directly related to the size of the nanoparticle, enabling nanoparticle size characterization. This method is based upon the use of a solution

dx.doi.org/10.1021/ac3031702 | Anal. Chem. 2013, 85, 473−486

of colloidal nanoparticles that is diluted to the point (i.e., pM nanoparticle concentration) where collisions of the nanoparticles with the electrode become a statistically random, and hence stochastic, process. Therefore, one cannot treat the current response like the usual, ensemble-based electrochemical current caused by an average of a large number of events. An effort has been made to describe the theory of these stochastic nanoparticle collisions.[110]

To date, the Bard lab has done several studies using this technique with a range of different electrodes, nanoparticles, and reactions of interest. These different experimental systems include: C electrode, Pt nanoparticles, and proton reduction;[109] C electrode, Pt nanoparticles, and hydrazine oxidation;[110] Au electrode, Pt nanoparticles, and hydrazine oxidation;[111] Pt electrode, IrO_x nanoparticles, and water oxidation;[112,113] and PtO_x electrode, Au nanoparticles, and sodium borohydride oxidation.[114] In these studies, two types of current responses have been found: the "staircase" and "blip". The staircase response is caused by a nanoparticle colliding with the UME, irreversibly sticking to it, and remaining electrocatalytically active. Therefore, the current goes up a step each collision, with the height of each step being the current associated with each nanoparticle collision. The blip response is caused by a nanoparticle colliding with the UME and either temporarily sticking to it or irreversibly sticking and becoming quickly deactivated. Therefore, the current associated with each nanoparticle is the height of each current spike (or blip) above the background current of the electrode.

The latest work from the Bard lab extends this technique to using potentiometric measurements to monitor single nanoparticles.[115] In this study, an Au UME was used to detect Pt nanoparticles, with the oxidation of hydrazine as the reaction of interest. Each nanoparticle collision with the electrode resulted in a change in the open circuit mixed potential of the electrode. This potentiometric technique was reported to have higher sensitivity, a simpler apparatus, and fewer problems with nanoparticle deactivation than its amperometric analogue.

Despite the usefulness of stochastic electrochemistry in size characterization of single nanoparticles, it has limitations when it comes to studying the in-depth structure−function relationship of single nanoparticles. Mainly, because the method is based on the random diffusion of nanoparticles in solution, researchers have no way of locating and imaging the nanoparticles to correlate the detailed structure of each particle to its current response. Additionally, one cannot obtain a full cyclic voltammogram from each nanoparticle, significantly limiting the amount of electrochemical information that can be gathered. This Review will now discuss a number of new techniques that show promise in obtaining a more complete understanding of the structure−function relationships of single electrocatalytic nanoparticles.

Single-Nanoparticle Electrochemistry. Kucernak and Chen were the first to report electrochemical properties of single nanoparticles using nanoelectrodes. These nanoparticles were fabricated by the direct electrodeposition of platinum onto carbon nanoelectrodes with radii under 50 nm.[116] This resulted in the formation of single polycrystalline Pt nanoparticles with a diameter of a few hundred nanometers on the tip of the electrodes. In two subsequent studies, the authors used these Pt nanoparticle electrodes to study the electrocatalysis of the oxygen reduction reaction and hydrogen oxidation reaction on the Pt nanoparticles. In the first study,[117] the authors showed that the size of the Pt nanoparticle catalyst has an effect on the mechanism of the oxygen reduction reaction. In the second study,[118] it was shown that hydrogen adsorption onto the Pt nanoparticle was the limiting step in hydrogen oxidation, thus demonstrating the complex kinetics of the reaction.

Our lab has been successful in studying the electrochemical response of single Au nanoparticles through the formation of a single-nanoparticle electrode (SNPE).[119] The SNPE was fabricated by chemically immobilizing a single Au nanoparticle (10−30 nm in diameter) onto a silane-modified Pt nanodisk electrode. The size of each nanodisk electrode was such that only a single Au nanoparticle could bind to it, enabling measurement of full cyclic voltammograms on a single Au nanoparticle. An advantage of this method in obtaining structure−function information about the nanoparticle is that, because the nanoparticle remains chemically attached to the electrode, it is easy to directly image it. However, due to the large size difference between the electrode glass insulation and the nanoparticle, high resolution imaging of the nanoparticle remains a challenge.

Steady-state cyclic voltammetry studies showed that the presence of a single Au nanoparticle greatly enhanced the limiting current over that obtained with a bare Pt electrode, signifying that the Au nanoparticle enhances the electron transfer from the Pt electrode to the redox molecules. The voltammetric response of Au SNPEs for the oxygen reduction reaction (ORR) was also studied. It was found that the Au SNPE had good electrocatalytic activity toward the ORR and that this electrocatalytic activity showed an Au nanoparticle size dependence. The ORR study showed both the ability of SPNEs to directly measure the catalytic activity of single Au nanoparticles and the type of useful structure−function information that can be gathered in single-nanoparticle electrocatalysis studies.

Mirkin and co-workers have developed an elegant method to image and examine electrode surfaces of single nanoelectrodes.[120] This method could provide detailed information about the electrode geometry and surface conditions. The Mirkin team has used this method to study the formation of single nanoparticles on a nanoelectrode during electrodeposition.[121] They have investigated the early stage during crystallization of single particles, which can be extremely useful for understanding electrochemical deposition of nanoparticles. This is an important method for many future studies involving detailed examination of the surface conditions of nanoelectrodes.

Plasmonic-Based Electrochemical Current Imaging. This recently developed technique by Tao and co-workers uses surface plasmon resonance (SPR) imaging to monitor the electrocatalytic reaction of single nanoparticles.[122] This technique, termed plasmonic-based electrochemical current imaging (P-ECi), obtains an electrochemical current by monitoring the conversion of a chemical species on a surface between its oxidized and reduced states. Changes in the local concentration of a species will alter the local refractive index, thus altering the SPR signal. This signal is directly related to the electrical current, enabling local current density imaging over the entire surface both quickly and noninvasively.[123] P-ECi enables determination of the electrocatalytic current of single nanoparticles as a function of time or voltage, with the latter enabling the recording of cyclic voltammograms of single nanoparticles.

In their most recent report,[122] Tao's team imaged the electrocatalytic activity of Pt nanoparticles toward the reduction of protons to dihydrogen. They were able to image the current density and obtain cyclic voltammograms of individual nanoparticles as small as 40 nm. Additionally, a microarray of printed Pt nanoparticles was created and P-ECi used to image the electrocatalytic activity of each printed nanoparticle spot toward proton reduction, demonstrating the technique's potential utility

dx.doi.org/10.1021/ac3031702 | Anal. Chem. 2013, 85, 473−486

in high-throughput nanoparticle catalyst screening. Despite the promise of this new technique, it may face limitations in observing the electrocatalytic current of very small (i.e., <5 nm) nanoparticles.[124] Additionally, as transmission electron microscopy (TEM) is used for detailed structural analysis of nanoparticles (which is essential to gaining structure−function knowledge), the samples would have to be made compatible with TEM.

Fluorescence Microscopy-Based Imaging. Developed by Chen and co-workers, this is a new and very useful technique that enables imaging the electrocatalysis of single nanoparticles.[125] It is based upon single-molecule fluorescence imaging of a molecule that becomes fluorescent upon reduction or oxidation at a nanoparticle surface. As one redox reaction results in the creation of one fluorescent molecule, this imaging can be done with single-reaction temporal resolution. The fluorescent imaging is done via total internal reflection fluorescence microscopy, enabling nanometer-scale spatial resolution and single-molecule sensitivity.

First reported to image electrocatalysis by single-walled carbon nanotubes,[126] the most recent report[125] by the Chen group uses the oxidation of Amplex Red to the fluorescence-active resorufin by H_2O_2 at gold nanorods (~21 nm diameter, ~150−700 nm length) to image single-nanoparticle electrocatalysis. Images with ~40 nm spatial resolution and single-reaction temporal resolution were reported. It was found that, despite having the same surface facets, the sides of the nanorods typically exhibit greater catalytic activity at the center, and this activity gradually decreases toward the ends. Additionally, it was found that the ratio of the catalytic activity of the center to the catalytic activity of the ends varied from nanorod to nanorod. This not only demonstrates the usefulness of this technique for single-nanoparticle electrocatalysis studies but also highlights the need for thorough structure−function characterization of single nanoparticles.

Scanning Electrochemical Cell Microscopy-Based Imaging. This technique, developed by Unwin and co-workers, uses scanning electrochemical cell microscopy (SECCM) to study heterogeneous electrocatalysis of single nanoparticles.[127] The spatial resolution of this technique is dependent upon the tip diameter of the probe. In this report, an ensemble of electrically connected Pt nanoparticles created via electrodeposition onto a single-walled carbon nanotube was studied. Specifically, the electrocatalytic activity of the nanoparticles toward the oxygen reduction and hydrogen evolution reactions was monitored. The technique enabled both the probing of the electrocatalytic activity of each individual nanoparticle (~100 nm diameter) in the ensemble and the determination of an overall map of the electrocatalytic activity of the entire ensemble. Currents as small as 10 fA (corresponding to the reduction of ~600 O_2 molecules under the authors' experimental conditions) could be detected at individual nanoparticles. The overall results showed that individual nanoparticles in the ensemble showed very different electrocatalytic activities despite being similarly sized.

SINGLE-MOLECULE ELECTROCHEMISTRY

Detection and analysis of single molecules represent the ultimate sensitivity in analytical chemistry. Single-molecule type experiments have several distinct advantages compared to bulk measurements including the ability to observe true and detailed reaction mechanisms and the ability to better understand molecular heterogeneity. A number of analytical techniques have been used to study single molecules. These include fluorescence microscopy, scanning probe microscopy, and patch clamp techniques. Detection and characterization of single redox molecules are intrinsically difficult and have only rarely been seen in the literature. This is largely due to technical challenges associated with measuring extremely small electrical signals. Conversely, single molecule detection with other analytical methods, especially florescence microscopy, is routine in many analytical chemistry laboratories. In this Review, we will emphasize experimental and theoretical work focusing on the faradaic response of single molecules. There are numerous extremely interesting reports on electrical conductance type experiments[128] that will not be included in this work.

Electrochemistry of Single Trapped Molecules. Bard and Fan first reported electrochemical detection of single redox molecules in solution.[129−131] Their method was based on the ultrafast diffusional transport of a single redox molecule trapped in a ~10 nm gap between two electrodes, one of which was a nanoelectrode used as an SECM probe while the other was a conductive substrate used as the counter electrode. A slight recess of ~10 nm was created at the end of the nanoelectrode probe such that a trap could be formed when the probe was brought in close vicinity to the indium tin oxide (ITO) substrate. The authors observed single molecule electrochemical behavior with a faradaic current on the order of ~1 pA corresponding to the molecule being repeatedly oxidized and reduced inside the trap at the two electrodes. This experiment was a clever design to gain a very large amplification of the single-molecule signal on the order of 10^7.

This strategy has recently been adapted by several research groups to investigate electrochemical responses of single redox molecules. Sun and Mirkin reported a study of single redox molecules trapped inside a nanometer-sized gap formed by bringing a slightly recessed glass nanopore electrode to the surface of a Hg electrode.[132] Their method enabled them to vary the number of the trapped redox molecules from one to hundreds. Both stochastic and steady state voltammetric behaviors were obtained with this method. Sun and Mirkin believe their method can be useful for further studying electron-transfer kinetics and double layer effects, among other things.

Lemay and co-workers have focused on a microfluidic strategy in which two electrodes are brought together within 100 nm in a microchannel, as shown in Figure 1c.[133,134] This distance can be well controlled during the microfabrication process. Fast redox cycling is obtained by flowing a solution of the redox molecules through the nanochannel and controlling the voltage applied on the electrode pairs. The electrochemical signal of a single redox molecule is recorded as a current pulse on the order of 50 fA. This current magnitude is much smaller than that recorded in Bard's experiment likely due to a larger electrode−electrode distance.

The White group has reported an interesting theoretical study of the voltammetric behavior of a single redox molecule trapped between a spherical nanoelectrode core and another spherical shell electrode using Brownian motion simulation.[135] The size of the core was kept at 20 nm whereas the distance was varied between 0.5 and 20 nm. This simulation was designed in a way to mimic the SECM trapping experiment of Fan and Bard. The authors simulated the steady-state current generated from a single molecule at each distance and found good agreement with experiments.

Single-Enzyme Electrochemistry. With advanced electronics, electrochemical methods can be used to access catalytic activity of single redox enzymes. In a recent report, Lemay and co-workers reported the direct measurement of the voltammetric

dx.doi.org/10.1021/ac3031702 | Anal. Chem. 2013, 85, 473−486

response of a redox protein catalyst, [NiFe]-hydrogenase.[136] In order to study protein electrochemistry, they first formed a film of the peptide polymyxin on a gold nanoelectrode, which they used to immobilize a submonolayer of [NiFe]-hydrogenase. They found that the adsorbed enzyme exhibited stable electrocatalytic behavior. The same procedure was scaled down in order to study catalytic behavior of a small number of protein molecules.[137] They used lithography to construct gold nanoelectrodes on which they attached less than 50 of these enzyme molecules. The Lemay group measured the electrocatalytic responses of an estimated 8 to 46 enzyme molecules. The key to observing electrochemical signal from such a small number of enzyme molecules is the very high turnover rate, ~1500−9000 s^{-1} for oxidation of H_2 at room temperature.

Gust and Moore and co-workers have examined the electrocatalytic activity of single [FeFe]-hydrogenase from *Clostridium acetobutylicum* (CaHydA).[138] This team has adapted a different strategy, using electrochemical scanning tunneling microscopy (STM) to study this interesting problem. They first formed a submonolayer of the enzyme CaHydA on an atomically flat gold electrode using a negatively charged self-assembled monolayer as a linker. They then measured the electrochemical response from an ensemble of surface immobilized enzymes catalyzing reduction of protons to dihydrogen and confirmed high catalytic activity. They used STM to estimate the surface density of proteins and calculated the turnover rate to be 21000 ± 12000 s^{-1} at neutral pH.

■ ELECTROCHEMISTRY FOR NANOMATERIALS

Track-Etched Nanoporous Membrane as Template. In templated synthesis, the dimensions of the desired structure are controlled by the template. Thus, control over template dimensions translates to control over structure dimensions, making this method attractive for the fabrication of nanoelectrodes/wires with controlled dimensions. Much of the work done involving nanoelectrode fabrication via templated synthesis has revolved around using nanoporous membranes as the template.[139] In the first report of this method, Penner and Martin electrochemically deposited Pt into the pores of a microporous polycarbonate membrane, creating an ensemble of Pt disk UMEs.[140] Most subsequent approaches have used either track-etched nanoporous polycarbonate membranes or nanoporous anodized alumina membranes as the templates.[141] In addition to electrochemical deposition, electroless deposition has also been used with this technique.[142] The use of nanoporous membranes as templates for the fabrication of nanoelectrode arrays has been extensively researched, and readers are referred to the literature cited within this section for more detailed information.

Block Copolymers as Template. More recently, much attention has been given to the use of self-assembled block copolymers as synthetic templates for many different types of nanostructures. Self-assembled block copolymers are simple to make and can display a wide range of different morphologies.[143,144] By removing one of the phases, they can serve as a template for various nanostructures. Russel et al. used a self-assembled diblock copolymer as a template for a nanowire array.[145] The researchers used polystyrene (PS) and polymethylmethacrylate (PMMA) to form a diblock copolymer consisting of hexagonally packed PMMA cylinders in a PS matrix. The PMMA was then removed to give a nanoporous array of PS. Co and Cu were then electrodeposited into these pores, resulting in vertical nanowire arrays with densities of over 1.9×10^{11} wires per cm^2. Ross et al. reported a different procedure using a self-assembled diblock copolymer to produce horizontal nanowire arrays with widths down to 9 nm.[146] The researchers used PS and polydimethylstyrene (PDMS) to form a monolayer of PDMS cylinders in a PS matrix. The PS was removed via oxygen plasma etching, leaving behind a template of PDMS cylinders onto which a metal was deposited using sputtering. The PDMS was then removed, leaving behind an array of metal nanowires.

Single Nanopore/Nanotube as Template. While the use of nanoporous membranes and self-assembled block copolymers as templates results in arrays of nanoelectrodes/wires, techniques have also been developed to template single nanoelectrodes/wires. Two of these will be highlighted here. The first, developed in our lab, uses a glass nanopore as a template for the fabrication of a single Au nanodisk electrode.[147] The glass nanopore is created by first fabricating a Pt nanodisk electrode via a laser-assisted micropipet pulling process. The Pt is then etched to create a Pt nanopore electrode. Au is then electrochemically deposited into this pore and polished, resulting in a Au nanodisk electrode as small as 4 nm in radius. This technique could be extended to create nanodisk electrodes of other metals, including Pd and Ag. The second technique we will highlight was reported by Unwin et al., in which single-walled carbon nanotubes (SWNTs) were used as templates for metal nanowires.[148] In this report, Au, Pt, and Pd nanowires were fabricated via electrodeposition onto SWNTs. The resulting nanowires were of submillimeter length and had heights as small as ~35 nm. A more thorough discussion of this paper is included in the nanoelectrode section of this Review.

■ NANOPORE ELECTROCHEMISTRY

Nanopore sensing is a widely used electroanalytical method for nanoparticle characterization based on the Coulter counter technique developed in the 1950s.[149] In this method, a potential is applied across a single nanometer-sized pore enclosed in an ultrathin material separating two compartments containing aqueous electrolyte solution. The ionic current through the nanopore is a function of the pore geometry and the solution conductivity and is measured as particles are driven through. As a particle moves through the pore, the ionic current is partially blocked, causing a temporary pulse in the current readout. The pulse amplitude can be directly correlated to the particle size, while the width of the pulse gives information about the translocation time and particle behavior inside the channel. The lasting popularity of the nanopore method can be attributed to its simple design, label-free nature, potential portability, and sensitivity to individual particles analyzed one at a time rather than in bulk. Since the 1970s when DeBlois first applied this approach to the detection of viruses and polystyrene particles as small as 90 nm in diameter,[150−152] it has been further expanded to detect everything from nanoparticles and small molecules to biological macromolecules such as proteins and DNA.[153−158] Different nanopore substrates and geometries provide different unique analytical capabilities. Here, we discuss these distinct approaches and explore recent advances in multiplexing and nanofluidics that promise to increase the speed, efficiency, and utility of electrochemical nanoparticle characterization.

Biological Nanopores. Nature has inspired the use of self-assembling protein ion channels with diameters as small as 2 nm. These pores can be reliably reproduced in lipid bilayers, and their tiny size enables them to detect very small molecules. Bezrukov and co-workers first employed these biological sensors to detect poly(ethylene glycol) polymers as small as 8 Å.[159] Since then, much work has been directed toward developing a nanopore

dx.doi.org/10.1021/ac3031702 | *Anal. Chem.* 2013, 85, 473−486

DNA sequencer. Kasianowicz et al. were able to determine the length of RNA and DNA molecules driven through an α-hemolysin pore based on translocation times calculated from the pulse widths,[160] while later work showed that the current blockages produced by different nucleotides could be distinguished from one another.[161−163] Similarly, other studies have investigated how pore geometry affects DNA entrance into the pore and have revealed information about the binding dynamics of DNA polymerase with DNA.[164] A substantial advantage of these biological nanopores is their ability to be easily modified to influence detection and binding specificity. Bayley and co-workers have increased nucleobase recognition at selected amino acid-modified recognition points within the nanopore[165,166] and increased temporal resolution by altering the charge in the pore to slow down DNA translocation.[167] This work has also been extended to other areas, with pores modified for detection of divalent metal ions, organic molecules, and proteins.[168−172] Recently, an aptamer-modified pore was employed to bind thrombin, producing a difference in the ionic current between bound and unbound states that enabled quantification of nanomolar analyte concentrations and offered important information about binding kinetics.[173] However, these biological pores are less stable and their size less flexible than their solid-state counterparts. Consequently, much research has also been conducted with solid-state nanopores of various materials.

Silicon Nitride Pores. Stable pores with diameters from 3 nm to hundreds of nm can be milled into silicon nitride using a focused ion/electron beam and, like biological pores, have also been used to study many aspects of DNA translocation. Golovchencko and co-workers first developed these pores, using the amplitudes and widths of current blockage events to distinguish between different DNA folding conformations[174−176] and reversing the polarity of the applied electric field to capture and repeatedly analyze the same DNA molecule to gain information about pore entrance and translocation dynamics.[177] Similarly, Dekker and co-workers have been able to distinguish between double- and single-stranded nucleic acid molecules based on their resulting current differences[178] and measure the electrical force on individual DNA molecules inside the pore.[179] Other significant advances have also been reported using these pores, including the development of a metal-oxide semiconductor preamplifier utilized in conjunction with the pore to increase temporal resolution, enabling detection of 1 μs events at signal bandwidths over 1 MHz.[180] Additionally, they have been used to distinguish between two different voltage-dependent mechanisms of translocation for electrically charged silica colloids.[181] Recent work has enabled solid-state pores to adapt some of the advantages of biological pores, including modification, to increase their versatility as biosensors. For example, a hybrid protein/solid-state nanopore has been created by inserting an α-hemolysin pore into a larger silicon nitride pore to draw on the advantages of both materials,[182] and silicon nitride pores modified with a gold surface have been functionalized with proteins to detect different antibodies based on current blockage pulse widths.[183]

Polymer and Glass Pores. Other solid-state materials have also been employed. Martin and co-workers have used conical pores track-etched in polymer membranes as a platform for detecting DNA, proteins, and even single porphyrin molecules.[184−187] These diameters can be as small as 4.5 nm, and the unique conical shape confines the sensing zone to a small area at the narrowest part of the cone, essentially shortening the pore length considerably. This effectively increases the electric field for the same applied potential, increasing particle frequency. Gold has also been deposited into these nanopores to form nanotubes that can be easily functionalized to detect proteins and investigate protein/antibody binding.[188,189] Conical glass nanopores developed by White and co-workers have yielded information about liposome and microgel deformation dynamics as they travel through the pore.[190−193] Similarly, conical quartz nanopipettes with diameters as small as 30 nm have been used to detect DNA folding and combined with optical tweezers to measure the electrophoretic force on DNA,[194,195] while similar silane-modified nanopipettes have been employed to detect reversible cobalt cation binding based on current rectification.[196] Likewise, our group has reported detection of DNA and polystyrene particles as small as 40 nm using cylindrical quartz nanochannels.[197]

Carbon Nanotubes and Graphene Nanopores. Carbon nanotube-based nanopores capable of determining the size, concentration, and surface charge of nanoparticles have been reported by Crooks and colleagues.[198−201] The short pore length ($\sim$1 μm) enables a large electric field to be produced at a relatively low applied potential, eliminating error caused by Brownian motion, while the interior walls are uncharged, ensuring that only electrophoretically driven flow can occur. With diameters in the range of 60−160 nm, these unique nanopores can be used to detect particles as small as 28 nm in diameter. The analyte concentration can be determined from pulse frequency, and they have shown that low and high surface charge particles can be distinguished by their pulse widths, with the higher surface charge corresponding to a higher electrophoretic mobility and faster translocation time. Graphene nanopores have also recently been fabricated as a novel new sensing platform.[202−205] Unlike other insulating nanopore materials, graphene is electrically conductive, robust, and ultrathin, which is ideal for DNA detection, as nucleotide bases can theoretically enter the pore one at a time to produce individual current blockage events. Fabrication involves using a TEM to drill pores ranging from 2 to 40 nm in diameter into a monolayer or multilayer sheet of graphene placed over a silicon nitride pore. DNA has been successfully driven through these nanopores to produce characteristic current blockades. Unlike other nanopore substrates, graphene has in-plane conductivity that is particularly sensitive to surface chemistry, also making it a promising new material for chemical sensors. Indeed, other nanopore sensing designs have already taken advantage of the increased temporal resolution provided by monitoring the transverse current rather than the ionic current through a pore. Tsutsui et al. have been able to electrically break a thin layer of gold in a 15 nm silicon dioxide pore to create a 0.8 nm gap between two gold electrodes capable of measuring the transverse tunneling current as individual DNA nucleotides travel through.[206] Although not currently able to accurately read long pieces of DNA, improvements to this design could render it capable of DNA sequencing in the future.

Tunable Nanopores. Recently, enhanced detection versatility has been reported using elastomeric nanopores with tunable diameters that can be adjusted in situ to detect or block different analytes based on size. Sowerby, Willmott, and Trau have fabricated conical nanopores with diameters of 30 nm and above in thermoplastic polyurethane using tungsten needles, enabling alteration of diameter size by mechanically stretching the membrane to detect polystyrene particles, adenoviruses, and individual and aggregated magnetic beads.[207−213] These pores also decrease the detrimental impact of clogging, as they can be stretched to release the blockage, and they could play a key role in

dx.doi.org/10.1021/ac3031702 | Anal. Chem. 2013, 85, 473−486

the development of adaptable biosensors. Recently, an agglutination assay was reported in which these adjustable pores were used to detect aggregation of functionalized metal rods triggered by biotin/avidin interactions by analyzing current blockages and durations, which could lead to faster multiplexed detection.[214]

Microfluidic and Multiplexed Signal Detection. Microfluidic devices and multiplexed signal detection increase the speed and efficiency of detection and could lead to ultrafast characterization of many types of nanostructures. Cleland and co-workers have reported a microfluidic nanoparticle analyzer capable of detecting 500 000 particles per second,[215] while Saleh and Sohn have created a microfluidic device comprising a nanopore in a PDMS slab sealed to a glass substrate with prepatterned electrodes.[216] These devices have been used to characterize antibody−antigen binding interactions based on differences in current blockage magnitudes[217] and have been modified with proteins to distinguish cells based on surface receptors,[218] since the blockage duration is increased when a cell slows down to interact with the receptors. Small solution reservoirs require low volumes of analyte, and the devices could be integrated into arrays for more efficient detection. Small micropore arrays have already been fabricated.[219] For example, Zhe and Carletta have developed a detection device with four microchannels in order to improve counting efficiency and quickly differentiate between PMMA and pollen particles.[220−222] They were able to measure detection in all channels using a single multiplexed signal and only one electronic detection setup, which could enable coupling of many channels for faster analysis. Jacobson and co-workers have reported a nanofluidic device with two 50 nm diameter nanopores in series on a silicon wafer, enabling the same hepatitis B virus capsid to be analyzed twice and giving information about physical properties such as electrophoretic mobility by measuring the time it takes to travel between the pores.[223] More pores could be added, providing an increased signal-to-noise ratio and more accurate statistics.

Both biological and solid-state nanopore devices have been fabricated from a variety of substrates to detect and characterize nanoparticles using the resistive-pulse method. Different materials provide different benefits, enhancing the versatility of this method. Recent advances in multiplexed and integrated microfluidic device technology promise to increase the speed and efficiency of analysis, ensuring the continued analytical importance of this technique.

■ NANOSCALE ELECTROCHEMICAL IMAGING

The ability to reveal electrochemical heterogeneity with nanoscale spatial resolution is important for a wide variety of chemical and biological applications, such as catalysis, transport, and neurochemistry. Electrochemical imaging has thus become increasingly important. Current research has been primarily focused on scanning probe-based imaging techniques, such as scanning electrochemical microscopy (SECM), but new electrochemical imaging techniques have also emerged in recent years that show enormous potential.

SECM is an extremely useful electrochemical technique developed in the Bard laboratory in 1989. In the last 20 years, SECM has gained enormous popularity in a wide variety of research areas including fundamental electrochemistry, bioanalytical chemistry, catalyst screening, corrosion studies, and molecular transport. SECM utilizes an UME or a nanoelectrode, which is scanned over a surface of interest. The microelectrode probe collects the electrochemical signal at each location, which reveals unique localized electrochemical information pertaining to the substrate. The spatial resolution of SECM depends largely on the size of the electrode probe, and significant progress has been achieved in the SECM community over the last several years to achieve nanoscale spatial resolution using this technique.

Achieving Nanoscale Spatial Resolution with Nanoelectrodes. A critical factor limiting the spatial resolution of SECM is the size of the electrode probe. Schuhmann and co-workers are among the first to use Pt nanoelectrodes in SECM to achieve ultrahigh spatial resolution.[224] In their 2004 report, they pointed out that one of the challenges of the use of nanoelectrodes as SECM probes is the difficulty maintaining a very small distance between the probe and the substrate, which is roughly several times the diameter of the electroactive surface. Mirkin's group has done outstanding research using nanoelectrode and nanopipette probes to achieve nanoscale spatial resolution using SECM. In a recent report, Mirkin and co-workers demonstrated nanoscale spatial resolution with both regular SECM and glass nanopipettes.[225] With sharp nanoelectrode probes on the order of 100 nm, they acquired lateral resolution of tens of nanometers. Figure 1d displays an SECM image of a CD surface imaged with a 190 nm sharp Pt tip. Although the smallest feature size they imaged was about 200 nm, they pointed out that, with proper nanoelectrode probes, lateral resolution on the order of 10 nm should be attainable.

The Amemiya group has pioneered the use of SECM to image one-dimensional nanostructures on insulating surfaces.[226−228] In a recent report,[229] Amemiya and co-workers used SECM to image and resolve individual single-walled carbon nanotubes (SWNTs) deposited on an insulating SiO_2 surface. In this experiment, they used an SECM probe between 1 and 10 μm, which is significantly larger than the diameter of the carbon nanotube. They proposed that a positive feedback mechanism might be responsible for the effective imaging of such a small feature on a large surface: when the SECM probe is brought in close vicinity to the SWNT, oxidized redox species are reduced back at the carbon nanotube surfaces giving rise to an enhancement of the tip current. Matysik and co-workers have also reported the use of Pt nanoelectrodes to image nanoporous Si/SiO_2 surfaces and the surface of biological cells. With sharp nanoelectrodes on the order of 100 nm, these authors obtained submicrometer spatial resolution.[230]

Nanoscale Imaging with Nanopipettes. There are two distinct imaging methods reported using ultrasharp glass/quartz nanopipette probes. The first method is scanning ion-conductance microscopy (SICM), which involves the use of a scanning glass nanopipette containing the same electrolyte solution as the bulk. The ionic current through the nanopipette is monitored as it scanned over the surface of interest. Very high spatial resolution and rich chemical/physical information can be obtained with SICM.[231−234] Readers are referred to an excellent review by Baker and co-workers.[235] The second imaging method uses a glass nanopipette filled with an electrolyte solution immiscible with the bulk solution, thus forming an electrolyte/electrolyte interface at the nanopipette orifice. The Mirkin group compared the imaging performance of ion-transfer mode SECM and found that the spatial resolution of the ion-transfer mode SECM was comparable to or better than the nanoelectrode-based SECM under these conditions.

The Amemiya group has also achieved nanoscale spatial resolution in SECM imaging using a pipet probe with sub-20 nm dimensions.[236] In this work, they used SECM to investigate molecular transport through a nanoporous Si membrane. The nanopipette was so small that extremely high spatial resolution

dx.doi.org/10.1021/ac3031702 | Anal. Chem. 2013, 85, 473−486

on the order of 30 nm was obtained to image individual nanopores in the membrane. On the basis of this exciting result, the Amemiya team anticipated that they could use the same technique to image biological nanopores in cellular membranes. Mirkin's group has reported a polishing procedure to reduce the surface roughness of the laser pulled glass nanopipettes.[237] The procedure they use is similar to the earlier polishing method they used to fabricate Pt and Au nanoelectrodes. The reduction in surface roughness is necessary in this specific imaging mode as it can help minimize and maintain the tip/substrate distance. However, the polishing has to be well controlled due to the extremely small physical dimension of the sharp glass tip.

A big motivation of achieving nanoscale spatial resolution in SECM imaging is the ability to study biological samples, especially individual biological cells. There have been several excellent articles published on this topic including a recent report from the Mirkin group[238] and several review articles.[239] Takahashi et al. have recently published an interesting article describing the use of voltage-switching mode SECM to image single neuronal cells.[240] They used a single SECM nanoelectrode, between 6 and 100 nm in radius, to simultaneously acquire high-quality topographical and electrochemical images of living cells. This imaging mode is based on switching the voltage of the nanoelectrode to change the faradaic current from a hindered diffusion feedback signal to the electrochemical measurement of interest. Additionally, this team measured neurotransmitter release from single PC12 cells using a relatively large (~6 μm) carbon microelectrode. The detection was carried out in a similar fashion to conventional single-cell amperometry with 650 mV constant voltage applied at the electrode with respect to a Ag/AgCl reference electrode. The secretion was stimulated with a high concentration K^+ solution.

Several other imaging techniques have been combined with SECM measurements in order to acquire additional surface information. These techniques include AFM and SICM.[241] In AFM-SECM imaging developed by Macpherson and Unwin,[15] a sharp nanoelectrode is used for both electrochemical current collection and force measurements. As such, both high-resolution topographical information and rich electrochemical information can be obtained simultaneously.

PERSPECTIVES

Nanoscale electrochemistry has played a critical role in gaining a deeper understanding of electron-transfer processes at the electrode/electrolyte interface and will continue to promote both fundamental and applied electrochemical research. Nanoelectrodes are of central importance in almost all aspects of nanoscale electrochemistry, from understanding electron-transfer kinetics and probing single catalytic nanoparticles to nanoscale electrochemical imaging. The use of nanoelectrodes will continue to increase in these research areas. Key challenges in nanoscale electrochemistry have been the lack of sufficient structural control in nanoelectrode preparation and the need for advanced methods for detailed structural characterization. These can be largely addressed by use of nanofabrication and nanocharacterization methods. Nanopore-based electrochemical methods have attracted considerable research interest and will likely continue to grow rapidly in the near future. We anticipate that nanopore-based sensors can be used in conjunction with other analytical methods, such as fluorescence and nanoelectrodes, to yield many new exciting results.

AUTHOR INFORMATION

Notes

The authors declare no competing financial interest.

Biographies

Stephen M. Oja is currently a graduate student in the Department of Chemistry at the University of Washington. He received his B.S. in chemistry from the University of Wisconsin—Madison in 2012, where he did atmospheric chemistry-related research for Dr. Frank Keutsch's group. He was a 2011 Amgen Scholar, completing a summer of research with Dr. Bo Zhang at the University of Washington before returning to the group for his PhD studies. His current research interests include developing new electrochemical techniques to do single-nanoparticle and single-molecule electrochemistry.

Marissa Wood received her B.A. in chemistry from Boston University in 2005. She worked at two different biotech companies in the Boston area before coming to graduate school at the University of Washington in 2008. She is currently a graduate student in Bo Zhang's lab investigating nanoparticle characterization using silica nanopores and new nanoelectrode fabrication methods.

Bo Zhang is currently an Assistant Professor in the Department of Chemistry at the University of Washington. He received his B.S. from Shandong University and his M.S. from Peking University both in China. He was awarded his PhD at University of Utah with Professor Henry S. White. He was a postdoc in the laboratory of Professor Andrew Ewing at the Pennsylvania State University before joining UW in 2008. His current research interests include understanding structure–function relationships of nanoparticle electrocatalysis, single-molecule electrocatalysis and electrochemistry, and electrochemical imaging of single neurons and their network.

ACKNOWLEDGMENTS

We are grateful for financial support from the National Science Foundation (CHE-1212805) and U.S. Defense Threat Reduction Agency (Contract No. HDTRA1-11-1-0005). We also acknowledge co-workers who have previously contributed to the work cited in this Review.

REFERENCES

(1) Wightman, R. M. *Anal. Chem.* **1981**, *53*, 1125A–1134A.
(2) Dayton, M. A.; Ewing, A. G.; Wightman, R. M. *Anal. Chem.* **1980**, *52*, 2392–2396.
(3) Dayton, M. A.; Brown, J. C.; Stutts, K. J.; Wightman, R. M. *Anal. Chem.* **1980**, *52*, 946–950.
(4) Bond, A. M.; Fleischmann, M.; Robinson, J. *J. Electroanal. Chem.* **1984**, *168*, 299–312.
(5) Kittlesen, G. P.; White, H. S.; Wrighton, M. S. *J. Am. Chem. Soc.* **1984**, *106*, 7389–7396.
(6) Wehmeyer, K. R.; Deakin, M. R.; Wightman, R. M. *Anal. Chem.* **1985**, *57*, 1913–1916.
(7) Bond, A. M. *J. Phys. Chem.* **1986**, *90*, 2911–2917.
(8) Morris, R.; Franta, D. J.; White, H. S. *J. Phys. Chem.* **1987**, *91*, 3559–3564.
(9) Wu, W. Z.; Huang, W. H.; Wang, W.; Wang, Z. L.; Cheng, J. K.; Xu, T.; Zhang, R. Y.; Chen, Y.; Liu, J. *J. Am. Chem. Soc.* **2005**, *127*, 8914–8915.
(10) Adams, K. L.; Puchades, M.; Ewing., A. G. *Annu. Rev. Anal. Chem.* **2008**, *1*, 329–355.
(11) Li, Z. Y.; Zhou, W.; Wu, Z. X.; Zhang, R. Y.; Xu, T. *Biosens. Bioelectron.* **2009**, *24*, 1358–1364.
(12) Fan, F. R. F.; Bard, A. J. *Science* **1995**, *10*, 871–874.
(13) Fan, F. R. F.; Kwak, J.; Bard, A. J. *J. Am. Chem. Soc.* **1996**, *118*, 9669–9675.

(14) Bard, A. J.; Mirkin, M. V. *Scanning Electrochemical Microscopy*, 2nd ed.; Marcel Dekker: New York, 2012.
(15) Macpherson, J. V.; Unwin, P. R. *Anal. Chem.* **2000**, *72*, 276−285.
(16) Kranz, C.; Friedbacher, G.; Mizaikoff, B.; Lugstein, A.; Smoliner, J.; Bertagnolli, E. *Anal. Chem.* **2001**, *73*, 2491−2500.
(17) Amatore, C.; Maisonhaute, E. *Anal. Chem.* **2005**, *77*, 305A−311A.
(18) Zhou, X. S.; Liu, L.; Fortgang, P.; Lefevre, A. S.; Serra-Muns, A.; Raouafi, N.; Amatore, C.; Mao, B. W.; Maisonhaute, E.; Schöllhorn, B. *J. Am. Chem. Soc.* **2011**, *133*, 7509−7516.
(19) Wipf, D. O.; Wightman, R. M. *J. Phys. Chem.* **1989**, *93*, 4286−8291.
(20) Wightman, R. M.; Wipf, D. O. *Acc. Chem. Res.* **1990**, *23*, 64−70.
(21) Amatore, C.; Maisonhaute, E.; Simonneau, G. *Electrochem. Commun.* **2000**, *2*, 81−84.
(22) Amatore, C.; Maisonhaute, E.; Simonneau, G. *J. Electroanal. Chem.* **2000**, *486*, 141−155.
(23) Guo, Z. Y.; Jiang, X. H.; Lin, X. Q. *Anal. Sci.* **2005**, *21*, 101−105.
(24) Guo, Z. Y.; Lin, X. Q. *J. Electroanal. Chem.* **2004**, *568*, 45−53.
(25) Zhang, Y. H.; Zhang, B.; White, H. S. *J. Phys. Chem. B* **2006**, *110*, 1768−1774.
(26) Watkins, J. J.; Chen, J.; White, H. S.; Abruña, H. D.; Maisonhaute, E.; Amatore, C. *Anal. Chem.* **2003**, *75*, 3962−3971.
(27) Sun, P.; Mirkin, M. V. *Anal. Chem.* **2006**, *78*, 6526−6534.
(28) Murray, R. W. *Chem. Rev.* **2008**, *108*, 2688−2720.
(29) Zoski, C. G. *Electroanalysis* **2002**, *14*, 1041−1051.
(30) Arrigan, D. W. M. *Analyst* **2004**, *129*, 1157−1165.
(31) Cox, J. T.; Zhang, B. *Annu. Rev. Anal. Chem.* **2012**, *5*, 253−272.
(32) Shao, Y.; Mirkin, M. V.; Fish, G.; Kokotov, S.; Palanker, D.; Lewis, A. *Anal. Chem.* **1997**, *69*, 1627−1634.
(33) Li, Y.; Bergman, D.; Zhang, B. *Anal. Chem.* **2009**, *81*, 5496−5502.
(34) Katemann, B. B.; Schuhmann, W. *Electroanalysis* **2002**, *14*, 22−28.
(35) Guerrette, J. P.; Oja, S. M.; Zhang, B. *Anal. Chem.* **2012**, *84*, 1609−1616.
(36) Penner, R. M.; Heben, M. J.; Lewis, N. S. *Anal. Chem.* **1989**, *61*, 1630−1636.
(37) Penner, R. M.; Heben, M. J.; Longin, T. L.; Lewis, N. S. *Science* **1990**, *250*, 1118−1121.
(38) Bach, C. E.; Nichols, R. J.; Beckmann, W.; Meyer, H.; Schulte, A.; Besenhard, J. O.; Jannakoudakis, P. D. *J. Electrochem. Soc.* **1993**, *140*, 1281−1284.
(39) Slevin, C. J.; Gray, N. J.; Macpherson, J. V.; Webb, M. A.; Unwin, P. R. *Electrochem. Commun.* **1999**, *1*, 282−288.
(40) Sun, P.; Zhang, Z.; Guo, J.; Shao, Y. *Anal. Chem.* **2001**, *73*, 5346−5351.
(41) Liu, B.; Rolland, J. P.; DeSimone, J. M.; Bard, A. J. *Anal. Chem.* **2005**, *77*, 3013−3017.
(42) Mirkin, M. V.; Fan, F. R. F.; Bard, A. J. *J. Electroanal. Chem.* **1992**, *328*, 47−62.
(43) Morris, R. B.; Franta, D. J.; White, H. S. *J. Phys. Chem.* **1987**, *91*, 3559−3564.
(44) Caston, S. L.; McCarley, R. L. *J. Electroanal. Chem.* **2002**, *529*, 124−134.
(45) MacFarlane, D. R.; Wong, D. K. Y. *J. Electroanal. Chem.* **1985**, *185*, 197−202.
(46) Lin, Y.; Trouillon, R.; Svensson, M. I.; Keighron, J. D.; Cans, A.-S.; Ewing, A. G. *Anal. Chem.* **2012**, *84*, 2949−2954.
(47) Lau, Y. Y.; Abe, T.; Ewing, A. G. *Anal. Chem.* **1992**, *64*, 1702−1705.
(48) Macpherson, J. V.; Jones, C. E.; Unwin, P. R. *J. Phys. Chem. B* **1998**, *102*, 9891−9897.
(49) Zhang, B.; Zhang, Y.; White, H. S. *Anal. Chem.* **2004**, *76*, 6229−6238.
(50) Zhang, B.; Galusha, J.; Shiozawa, P. G.; Wang, G.; Bergren, A. J.; Jones, R. M.; White, R. J.; Ervin, E. N.; Cauley, C. C.; White, H. S. *Anal. Chem.* **2007**, *79*, 4778−4787.
(51) Sun, P. *Anal. Chem.* **2010**, *82*, 276−291.
(52) Bard, A. J.; Faulkner, L. R. *Electrochemical Methods*, 2nd ed.; John Wiley & Sons: New York, 2001.
(53) Xu, Q.; Rioux, R. M.; Dickey, M. D.; Whitesides, G. M. *Acc. Chem. Res.* **2007**, *41*, 1566−1577.
(54) Lipomi, D. J.; Martinez, R. V.; Whitesides, G. M. *Angew. Chem., Int. Ed.* **2011**, *50*, 8566−8583.
(55) Lipomi, D. J.; Martinez, R. V.; Rioux, R. M.; Cademartiri, L.; Reus, W. F.; Whitesides, G. M. *ACS Appl. Mater. Interfaces* **2010**, *2*, 2503−2514.
(56) Xu, Q.; Gates, B. D.; Whitesides, G. M. *J. Am. Chem. Soc.* **2004**, *126*, 1332−1333.
(57) Dickey, M. D.; Lipomi, D. J.; Bracher, P. J.; Whitesides, G. M. *Nano Lett.* **2008**, *8*, 4568−4575.
(58) Dawson, K.; Strutwolf, J.; Rodgers, K. P.; Herzog, G.; Arrigan, D. W. M.; Quinn, A. J.; O'Riordan, A. *Anal. Chem.* **2011**, *83*, 5535−5540.
(59) Menke, E. J.; Thompson, M. A.; Xiang, C.; Yang, L. C.; Penner, R. M. *Nat. Mater.* **2006**, *5*, 914−919.
(60) Xiang, C.; Kung, S. C.; Taggart, D. K.; Yang, F.; Thompson, M. A.; Güell, A. G.; Yang, Y.; Penner, R. M. *ACS Nano* **2008**, *2*, 1939−1949.
(61) Yang, Y.; Kung, S. C.; Taggart, D. K.; Xiang, C.; Yang, F.; Brown, M. A.; Güell, A. G.; Kruse, T. J.; Hemminger, J. C.; Penner, R. M. *Nano Lett.* **2008**, *8*, 2447−2451.
(62) Hujdic, J. E.; Taggart, D. K.; Kung, S. C.; Menke, E. J. *J. Phys. Chem. Lett.* **2010**, *1*, 1055−1059.
(63) Kung, S. C.; van der Veer, W. E.; Yang, F.; Donavan, K. C.; Penner, R. M. *Nano Lett.* **2010**, *10*, 1481−1485.
(64) Hujdic, J. E.; Sargisian, A. P.; Shao, J.; Ye, T.; Menke, E. J. *Nanoscale* **2011**, *3*, 2697−2699.
(65) Dudin, P. V.; Snowden, M. E.; Macpherson, J. V.; Unwin, P. R. *ACS Nano* **2011**, *12*, 10017−10025.
(66) Delmastro, J. R.; Smith, D. E. *J. Phys. Chem.* **1967**, *71*, 2138−2149.
(67) Bond, A. M.; Oldham, K. B. *J. Electroanal. Chem.* **1983**, *158*, 193−215.
(68) Saito, Y. *Rev. Polarogr. (Jpn.)* **1968**, *15*, 177−187.
(69) Oldham, K. B.; Zoski, C. G. *J. Electroanal. Chem.* **1988**, *256*, 11−19.
(70) Watkins, J. J.; Zhang, B.; White, H. S. *J. Chem. Educ.* **2005**, *82*, 712−719.
(71) Thakar, R.; Wilburn, J. P.; Baker, L. A. *Electroanalysis* **2011**, *23*, 1543−1547.
(72) Agyekum, I.; Nimley, C.; Yang, C. X.; Sun, P. *J. Phys. Chem. C* **2010**, *114*, 14970−14974.
(73) Feldberg, S. W. *Anal. Chem.* **2010**, *82*, 5176−5183.
(74) Marcus, R. A. *Annu. Rev. Phys. Chem.* **1964**, *15*, 155−196.
(75) Marcus, R. A. *J. Chem. Phys.* **1965**, *43*, 679−701.
(76) Hush, N. S. *J. Electroanal. Chem.* **1999**, *470*, 170−195.
(77) Chidsey, C. E. D. *Science* **1991**, *215*, 919−922.
(78) Amatore, C.; Fosset, B.; Bartlet, J.; Deakin, M. R.; Wightman, R. M. *J. Electroanal. Chem.* **1988**, *256*, 255−268.
(79) Amatore, C.; Deakin, M. R.; Wightman, R. M. *J. Electroanal. Chem.* **1987**, *220*, 49−63.
(80) Norton, J. D.; White, H. S.; Feldberg, S. W. *J. Phys. Chem.* **1990**, *94*, 6772−6780.
(81) Norton, J. D.; Benson, W. E.; White, H. S.; Pendley, B.; Abruna, H. D. *Anal. Chem.* **1991**, *63*, 1909−1914.
(82) Lee, C.; Anson, F. C. *J. Electroanal. Chem.* **1992**, *323*, 381.
(83) Maeda, M.; McClure, D. J.; White, H. S. *J. Electroanal. Chem.* **1986**, *200*, 383−387.
(84) Seibold, J. D.; Scott, E. R.; White, H. S. *J. Electroanal. Chem.* **1989**, *264*, 281−289.
(85) Conyers, J. L.; White, H. S. *Anal. Chem.* **2000**, *72*, 4441−4446.
(86) Watkins, J. J.; Cope, B. D.; Conyers, J., Jr.; White, H. S. In *Interfaces, Phenomena, and Nanostructures in Lithium Batteries*; Klingler, R., Ed.; Electrochemical Society: Princeton, NJ, 2001; Vol. *2001−36*, p 163.
(87) Chen, S. L; Kucernak, A. *Electrochem. Commun.* **2002**, *4*, 80−85.
(88) Chen, S. L; Kucernak, A. *J. Phys. Chem. B* **2002**, *106*, 9396−9404.
(89) Smith, C. P.; White, H. S. *Anal. Chem.* **1993**, *65*, 3343−3353.
(90) Watkins, J. J.; White, H. S. *Langmuir* **2004**, *20*, 5474−5483.
(91) Liu, Y. W.; Zhang, Q. F.; Chen, S. L. *Electrochim. Acta* **2010**, *55*, 8280−8286.

(92) Liu, Y. W.; Chen, S. L. *J. Phys. Chem. C* **2012**, *116*, 13594−13602.
(93) Liu, Y. W.; He, R.; Zhang, Q. F.; Chen, S. L. *J. Phys. Chem. C* **2010**, *114*, 10812−10822.
(94) Sun, Y.; Liu, Y. W.; Liang, Z. X.; Xiong, L.; Wang, A. L.; Chen, S. L. *J. Phys. Chem. C* **2009**, *113*, 9878−9883.
(95) He, R.; Chen, S. L.; Yang, F.; Wu, B. L. *J. Phys. Chem. B* **2006**, *110*, 3262−3270.
(96) Bell, A. T. *Science* **2003**, *299*, 1688−1691.
(97) Vajda, S.; Pellin, M. J.; Greeley, J. P.; Marshall, C. L.; Curtiss, L. A.; Ballentine, G. A.; Elam, J. W.; Catillon-Mucherie, S.; Redfern, P. C.; Mehmood, F.; Zapol, P. *Nat. Mater.* **2009**, *8*, 213−216.
(98) Crooks, R. M.; Zhao, M. Q.; Sun, L.; Chechik, V.; Yeung, L. K. *Acc. Chem. Res.* **2001**, *34*, 181−190.
(99) Ye, H.; Crooks, R. M. *J. Am. Chem. Soc.* **2005**, *127*, 4930−4934.
(100) Wang, C.; Daimon, H.; Lee, Y.; Kim, J.; Sun, S. *J. Am. Chem. Soc.* **2007**, *129*, 6974−6975.
(101) Lim, B.; Jiang, M.; Camargo, P. H. C.; Cho, E. C.; Tao, J.; Lu, X.; Zhu, Y.; Xia, Y. *Science* **2009**, *324*, 1302−1305.
(102) Kumar, S.; Zhou, S. *Langmuir* **2009**, *25*, 574−581.
(103) Ye, H.; Crooks, R. M. *J. Am. Chem. Soc.* **2007**, *129*, 3627−3633.
(104) Templeton, A. C.; Wuelfing, M. P.; Murray, R. W. *Acc. Chem. Res.* **2000**, *33*, 27−36.
(105) Murray, R. W. *Chem. Rev.* **2008**, *108*, 2688−2720.
(106) Brust, M.; Walker, M.; Bethell, D.; Schiffrin, D. J.; Whyman, R. *J. Chem. Soc., Chem. Commun.* **1994**, 801−802.
(107) Tang, Z. H.; Xu, B.; Wu, B. H.; Germann, M. W.; Wang, G. L. *J. Am. Chem. Soc.* **2010**, *132*, 3367−3374.
(108) Xiao, X.; Bard, A. J. *J. Am. Chem. Soc.* **2007**, *129*, 9610−9612.
(109) Xiao, X.; Fan, F.-R. F.; Zhou, J.; Bard, A. J. *J. Am. Chem. Soc.* **2008**, *130*, 16669−16677.
(110) Kwon, S. J.; Zhou, H.; Fan, F.-R. F.; Vorobyev, V.; Zhang, B.; Bard, A. J. *Phys. Chem. Chem. Phys.* **2011**, *13*, 5394−5402.
(111) Xiao, X.; Pan, S.; Jang, J. S.; Fan, F.-R. F.; Bard, A. J. *J. Phys. Chem. C* **2009**, *113*, 14978−14982.
(112) Kwon, S. J.; Fan, F.-R. F.; Bard, A. J. *J. Am. Chem. Soc.* **2010**, *132*, 13165−13167.
(113) Zhou, H.; Fan, F.-R. F.; Bard, A. J. *J. Phys. Chem. Lett.* **2010**, *1*, 2671−2674.
(114) Kwon, S. J.; Bard, A. J. *J. Am. Chem. Soc.* **2012**, *134*, 7102−7108.
(115) Zhou, H.; Park, J. H.; Fan, F.-R. F.; Bard, A. J. *J. Am. Chem. Soc.* **2012**, *134*, 13212−13215.
(116) Chen, S.; Kucernak, A. *J. Phys. Chem. B* **2003**, *107*, 8392−8402.
(117) Chen, S.; Kucernak, A. *J. Phys. Chem. B* **2004**, *108*, 3262−3276.
(118) Chen, S.; Kucernak, A. *J. Phys. Chem B* **2004**, *108*, 13984−13994.
(119) Li, Y.; Cox, J. T.; Zhang, B. *J. Am. Chem. Soc.* **2010**, *132*, 3047−3054.
(120) Nogala, W.; Velmurugan, J.; Mirkin, M. V. *Anal. Chem.* **2012**, *84*, 5192−5197.
(121) Velmurugan, J.; Noel, J.-M.; Nogala, W.; Mirkin, M. V. *Chem. Sci.* **2012**, *3*, 3307−3314.
(122) Shan, X.; Díez-Pérez, I.; Wang, L.; Wiktor, P.; Gu, Y.; Zhang, L.; Wang, W.; Lu, J.; Wang, S.; Gong, Q.; Li, J.; Tao, N. *Nat. Nanotechnol.* **2012**, *7*, 688−672.
(123) Shan, X.; Patel, U.; Wang, S.; Iglesias, R.; Tao, N. *Science* **2010**, *327*, 1363−1366.
(124) Percival, S. J.; Zhang, B. *Nat. Nanotechnol.* **2012**, *7*, 615−616.
(125) Zhou, X.; Andoy, N. M.; Liu, G.; Choudhary, E.; Han, K. -S.; Shen, H.; Chen, P. *Nat. Nanotechnol.* **2012**, *7*, 237−241.
(126) Xu, W.; Shen, H.; Kim, Y. J.; Zhou, X.; Liu, G.; Park, J.; Chen, P. *Nano Lett.* **2009**, *9*, 3968−3973.
(127) Lai, S. C. S.; Dudin, P. V.; Macpherson, J. V.; Unwin, P. R. *J. Am. Chem. Soc.* **2011**, *133*, 10744−10747.
(128) Tao, N. J. *Nat. Nanotechnol.* **2006**, *1*, 173−181.
(129) Fan, F. R. F.; Bard, A. J. *Science* **1995**, *267*, 871−874.
(130) Fan, F. R. F.; Kwak, J.; Bard, A. J. *J. Am. Chem. Soc.* **1996**, *118*, 9669−9675.
(131) Bard, A. J.; Fan, F. R. F. *Acc. Chem. Res.* **1996**, *29*, 572−578.
(132) Sun, P.; Mirkin, M. V. *J. Am. Chem. Soc.* **2008**, *130*, 8241−8250.
(133) Zevenbergen, M. A. G.; Singh, P. S.; Goluch, E. D.; Wolfrum, B. L.; Lemay, S. G. *Nano Lett.* **2011**, *11*, 2881−2886.
(134) Singh, P. S.; Chan, H.-S. M.; Kang, S.; Lemay, S. G. *J. Am. Chem. Soc.* **2011**, *133*, 18289−18295.
(135) White, R. J.; White, H. S. *Anal. Chem.* **2008**, *24*, 2850−2855.
(136) Hoeben, F. J. M.; Heller, I.; Albracht, S. P. J.; Dekker, C.; Lemay, S. G.; Heering, H. A. *Langmuir* **2008**, *24*, 5925−5931.
(137) Hoeben, F. J. M.; Meijer, F. S.; Dekker, C.; Albracht, S. P. J.; Heering, H. A.; Lemay, S. G. *ACS Nano* **2008**, *2*, 2497−2504.
(138) Madden, C.; Vaughn, M. D.; Díez-Pérez, I.; Brown, K. A.; King, P. W.; Gust, D.; Moore, A. L.; Moore, T. A. *J. Am. Chem. Soc.* **2012**, *134*, 1577−1582.
(139) Hulteen, J. C.; Martin, C. R. *J. Mater. Chem.* **1997**, *7*, 1075−1087.
(140) Penner, R. M.; Martin, C. R. *Anal. Chem.* **1987**, *59*, 2625−2630.
(141) Martin, C. R. *Science* **1994**, *266*, 1961−1966.
(142) Menon, V. P.; Martin, C. R. *Anal. Chem.* **1995**, *67*, 1920−1928.
(143) Bates, F. S.; Fredrickson, G. H. *Phys. Today* **1999**, *52*, 32−38.
(144) Simon, P.; Ulrich, R.; Spiess, H.; Wiesner, U. *J. Chem. Mater.* **2001**, *13*, 3463−3486.
(145) Thurn-Albrecht, T.; Schotter, J.; Kästle, G. A.; Emley, N.; Shibauchi, T.; Krusin-Elbaum, L.; Guarini, K.; Black, C. T.; Tuominen, M. T.; Russell, T. P. *Science* **2000**, *290*, 2126−2129.
(146) Jung, Y. S.; Lee, J. H.; Lee, J. Y.; Ross, C. A. *Nano Lett.* **2010**, *10*, 3722−3726.
(147) Jena, B. K.; Percival, S. J.; Zhang, B. *Anal. Chem.* **2010**, *82*, 6737−6743.
(148) Dudin, P. V.; Snowden, M. E.; Macpherson, J. V.; Unwin, P. R. *ACS Nano* **2011**, *5*, 10017−10025.
(149) Coulter, W. H. U.S. Patent 2656508, October 20, 1953.
(150) Deblois, R. W.; Bean, C. P. *Rev. Sci. Instrum.* **1970**, *41*, 909−916.
(151) Deblois, R. W.; Bean, C. P.; Wesley, R. K. A. *J. Colloid Interface Sci.* **1977**, *61*, 323−335.
(152) Deblois, R. W.; Wesley, R. K. A. *J. Virol.* **1977**, *23*, 227−233.
(153) Bayley, H.; Martin, C. R. *Chem. Rev.* **2000**, *100*, 2575−2594.
(154) Bayley, H.; Cremer, P. S. *Nature* **2001**, *413*, 226−230.
(155) Deamer, D. W.; Branton, D. *Acc. Chem. Res.* **2002**, *35*, 817−825.
(156) Henriquez, R. R.; Ito, T.; Sun, L.; Crooks, R. M. *Analyst* **2004**, *129*, 478−482.
(157) Kozak, D.; Anderson, W.; Vogel, R.; Trau, M. *Nano Today* **2011**, *6*, 531−545.
(158) Dekker, C. *Nat. Nanotechnol.* **2007**, *2*, 209−215.
(159) Bezrukov, S. M.; Vodyanoy, I.; Parsegian, V. A. *Nature* **1994**, *370*, 279−281.
(160) Kasianowicz, J. J.; Brandin, E.; Branton, D.; Deamer, D. W. *Proc. Natl. Acad. Sci. U.S.A.* **1996**, *93*, 13770−13773.
(161) Akeson, M.; Branton, D.; Kasianowicz, J. J.; Brandin, E.; Deamer, D. W. *Biophys. J.* **1999**, *77*, 3227−3233.
(162) Meller, A.; Nivon, L.; Brandin, E.; Golovchenko, J.; Branton, D. *Proc. Natl. Acad. Sci. U.S.A.* **2000**, *97*, 1079−1084.
(163) Vercoutere, W.; Winters-Hilt, S.; Olsen, H.; Deamer, D.; Haussler, D.; Akeson, M. *Nat. Biotechnol.* **2001**, *19*, 248−252.
(164) Henrickson, S. E.; Misakian, M.; Robertson, B.; Kasianowicz, J. J. *Phys. Rev. Lett.* **2000**, *85*, 3057−3060.
(165) Stoddart, D.; Heron, A. J.; Klingelhoefer, J.; Mikhailova, E.; Maglia, G.; Bayley, H. *Nano Lett.* **2010**, *10*, 3633−3637.
(166) Hammerstein, A. F.; Jayasinghe, L.; Bayley, H. *J. Biol. Chem.* **2011**, *286*, 14324−14334.
(167) Rincon-Restrepo, M.; Milthallova, E.; Bayley, H.; Maglia, G. *Nano Lett.* **2011**, *11*, 746−750.
(168) Gu, L. Q.; Braha, O.; Conlan, S.; Cheley, S.; Bayley, H. *Nature* **1999**, *398*, 686−690.
(169) Sanchez-Quesada, J.; Ghadiri, M. R.; Bayley, H.; Braha, O. *J. Am. Chem. Soc.* **2000**, *122*, 11757−11766.
(170) Bayley, H.; Braha, O.; Gu, L. Q. *Adv. Mater.* **2000**, *12*, 139−142.
(171) Movileanu, L.; Howorka, S.; Braha, O.; Bayley, H. *Nat. Biotechnol.* **2000**, *18*, 1091−1095.
(172) Howorka, S.; Cheley, S.; Bayley, H. *Nat. Biotechnol.* **2001**, *19*, 636−639.

(173) Rotem, D.; Jayasinghe, L.; Salichou, M.; Bayley, H. *J. Am. Chem. Soc.* **2012**, *134*, 2781−2787.
(174) Li, J.; Stein, D.; McMullan, C.; Branton, D.; Aziz, M. J.; Golovchenko, J. A. *Nature* **2001**, *412*, 166−169.
(175) Li, J. L.; Gershow, M.; Stein, D.; Brandin, E.; Golovchenko, J. A. *Nat. Mater.* **2003**, *2*, 611−615.
(176) Lu, B.; Albertorio, F.; Hoogerheide, D. P.; Golovchenko, J. A. *Biophys. J.* **2011**, *101*, 70−79.
(177) Gershow, M.; Golovchenko, J. A. *Nat. Nanotechnol.* **2007**, *2*, 775−779.
(178) Skinner, G. M.; van den Hout, M.; Broekmans, O.; Dekker, C.; Dekker, N. H. *Nano Lett.* **2009**, *9*, 2953−2960.
(179) Keyser, U. F.; Koeleman, B. N.; Van Dorp, S.; Krapf, D.; Smeets, R. M. M.; Lemay, S. G.; Dekker, N. H.; Dekker, C. *Nat. Phys.* **2006**, *2*, 473−477.
(180) Rosenstein, J. K.; Wanunu, M.; Merchant, C. A.; Drndic, M.; Shepard, K. L. *Nat. Methods* **2012**, *9*, 487−492.
(181) Bacri, L.; Oukhaled, A. G.; Schiedt, B.; Patriarche, G.; Bourhis, E.; Gierak, J.; Pelta, J.; Auvray, L. *J. Phys. Chem. B* **2011**, *115*, 2890−2898.
(182) Hall, A. R.; Scott, A.; Rotem, D.; Mehta, K. K.; Bayley, H.; Dekker, C. *Nat. Nanotechnol.* **2010**, *5*, 874−877.
(183) Wei, R.; Gatterdam, V.; Wieneke, R.; Tampe, R.; Rant, U. *Nat. Nanotechnol.* **2012**, *7*, 257−263.
(184) Baker, L. A.; Choi, Y.; Martin, C. R. *Curr. Nanosci.* **2006**, *2*, 243−255.
(185) Li, N. C.; Yu, S. F.; Harrell, C. C.; Martin, C. R. *Anal. Chem.* **2004**, *76*, 2025−2030.
(186) Harrell, C. C.; Choi, Y.; Horne, L. P.; Baker, L. A.; Siwy, Z. S.; Martin, C. R. *Langmuir* **2006**, *22*, 10837−10843.
(187) Heins, E. A.; Siwy, Z. S.; Baker, L. A.; Martin, C. R. *Nano Lett.* **2005**, *5*, 1824−1829.
(188) Sexton, L. T.; Horne, L. P.; Sherrill, S. A.; Bishop, G. W.; Baker, L. A.; Martin, C. R. *J. Am. Chem. Soc.* **2007**, *129*, 13144−13152.
(189) Sexton, L. T.; Mukaibo, H.; Katira, P.; Hess, H.; Sherrill, S. A.; Horne, L. P.; Martin, C. R. *J. Am. Chem. Soc.* **2010**, *132*, 6755−6763.
(190) Zhang, B.; Galusha, J.; Shiozawa, P. G.; Wang, G. L.; Bergren, A. J.; Jones, R. M.; White, R. J.; Ervin, E. N.; Cauley, C. C.; White, H. S. *Anal. Chem.* **2007**, *79*, 4778−4787.
(191) Holden, D. A.; Hendrickson, G.; Lyon, L. A.; White, H. S. *J. Phys. Chem. C* **2011**, *115*, 2999−3004.
(192) Holden, D. A.; Hendrickson, G. R.; Lan, W. J.; Lyon, L. A.; White, H. S. *Soft Matter* **2011**, *7*, 8035−8040.
(193) Lan, W. J.; Holden, D. A.; Liu, J.; White, H. S. *J. Phys. Chem. C* **2011**, *115*, 18445−18452.
(194) Steinbock, L. J.; Otto, O.; Chimerel, C.; Gornall, J.; Keyser, U. F. *Nano Lett.* **2010**, *10*, 2493−2497.
(195) Steinbock, L. J.; Otto, O.; Skarstam, D. R.; Jahn, S.; Chimerel, C.; Gornall, J. L.; Keyser, U. F. *J. Phys.: Condens. Matter* **2010**, *22*, 454113.
(196) Sa, N.; Fu, Y.; Baker, L. A. *Anal. Chem.* **2010**, *82*, 9963−9966.
(197) Zhang, B.; Wood, M.; Lee, H. *Anal. Chem.* **2009**, *81*, 5541−5548.
(198) Sun, L.; Crooks, R. M. *J. Am. Chem. Soc.* **2000**, *122*, 12340−12345.
(199) Ito, T.; Sun, L.; Crooks, R. M. *Anal. Chem.* **2003**, *75*, 2399−2406.
(200) Ito, T.; Sun, L.; Henriquez, R. R.; Crooks, R. M. *Acc. Chem. Res.* **2004**, *37*, 937−945.
(201) Ito, T.; Sun, L.; Bevan, M. A.; Crooks, R. M. *Langmuir* **2004**, *20*, 6940−6945.
(202) Garaj, S.; Hubbard, W.; Reina, A.; Kong, J.; Branton, D.; Golovchenko, J. A. *Nature* **2010**, *467*, 190−U73.
(203) Schneider, G. F.; Kowalczyk, S. W.; Calado, V. E.; Pandraud, G.; Zandbergen, H. W.; Vandersypen, L. M. K.; Dekker, C. *Nano Lett.* **2010**, *10*, 3163−3167.
(204) Merchant, C. A.; Healy, K.; Wanunu, M.; Ray, V.; Peterman, N.; Bartel, J.; Fischbein, M. D.; Venta, K.; Luo, Z.; Johnson, A. T. C.; Drndic, M. *Nano Lett.* **2010**, *10*, 2915−2921.
(205) Wells, D. B.; Belkin, M.; Comer, J.; Aksimentiev, A. *Nano Lett.* **2012**, *12*, 4117−4123.
(206) Tsutsui, M.; Rahong, S.; Iizumi, Y.; Okazaki, T.; Taniguchi, M.; Kawai, T. *Sci. Rep.* **2012**, *2*, 1−7.
(207) Sowerby, S. J.; Broom, M. F.; Petersen, G. B. *Sens. Actuators, B: Chem.* **2007**, *123*, 325−330.
(208) Willmott, G. R.; Moore, P. W. *Nanotechnology* **2008**, *19*, 475504.
(209) Willmott, G. R.; Vogel, R.; Yu, S. S. C.; Groenewegen, L. G.; Roberts, G. S.; Kozak, D.; Anderson, W.; Trau, M. *J. Phys.: Condens. Matter* **2010**, *22*, 454116.
(210) Vogel, R.; Willmott, G.; Kozak, D.; Roberts, G. S.; Anderson, W.; Groenewegen, L.; Glossop, B.; Barnett, A.; Turner, A.; Trau, M. *Anal. Chem.* **2011**, *83*, 3499−3506.
(211) Willmott, G. R.; Parry, B. E. T. *J. Appl. Phys.* **2011**, *109*, 094307.
(212) Willmott, G. R.; Platt, M.; Lee, G. U. *Biomicrofluidics* **2012**, *6*, 014103.
(213) Kozak, D.; Anderson, W.; Grevett, M.; Trau, M. *J. Phys. Chem. C* **2012**, *116*, 8554−8561.
(214) Platt, M.; Willmott, G. R.; Lee, G. U. *Small* **2012**, *8*, 2436−2444.
(215) Fraikin, J.-L.; Teesalu, T.; McKenney, C. M.; Ruoslahti, E.; Cleland, A. N. *Nat. Nanotechnol.* **2011**, *6*, 308−313.
(216) Saleh, O. A.; Sohn, L. L. *Nano Lett.* **2003**, *3*, 37−38.
(217) Saleh, O. A.; Sohn, L. L. *Proc. Natl. Acad. Sci. U.S.A.* **2003**, *100*, 820−824.
(218) Carbonaro, A.; Mohanty, S. K.; Huang, H.; Godley, L. A.; Sohn, L. L. *Lab Chip* **2008**, *8*, 1478−1485.
(219) Wu, Y.; Benson, J. D.; Critser, J. K.; Almasri, M. *J. Micromech. Microeng.* **2010**, *20*, 085035.
(220) Jagtiani, A. V.; Zhe, J.; Hu, J.; Carletta, J. *Meas. Sci. Technol.* **2006**, *17*, 1706−1714.
(221) Zhe, J.; Jagtiani, A.; Dutta, P.; Hu, J.; Carletta, J. *J. Micromech. Microeng.* **2007**, *17*, 304−313.
(222) Jagtiani, A. V.; Carletta, J.; Zhe, J. *J. Micromech. Microeng.* **2011**, *21*, 065004.
(223) Harms, Z. D.; Mogensen, K. B.; Nunes, P. S.; Zhou, K.; Hildenbrand, B. W.; Mitra, I.; Tan, Z.; Zlotnick, A.; Kutter, J. P.; Jacobson, S. C. *Anal. Chem.* **2011**, *83*, 9573−9578.
(224) Katemann, B. B.; Schulte, A.; Schuhmann, W. *Electroanalysis* **2004**, *16*, 60−65.
(225) Laforge, F. O.; Velmurugan, J.; Wang, Y.; Mirkin, M. V. *Anal. Chem.* **2009**, *81*, 3143−3150.
(226) Xiong, H.; Gross, D. A.; Guo, J.; Amemiya, S. *Anal. Chem.* **2006**, *78*, 1946−1957.
(227) Xiong, H.; Kim, J.; Kim, E.; Amemiya, S. *J. Electroanal. Chem.* **2009**, *629*, 78−86.
(228) Kim, E.; Kim, J.; Amemiya, S. *Anal. Chem.* **2009**, *81*, 4788−4791.
(229) Kim, J.; Xiong, H.; Hofmann, M.; Kong, J.; Amemiya, S. *Anal. Chem.* **2010**, *82*, 1605−1607.
(230) Bergner, S.; Palatzky, P.; Wegener, J.; Matysik, F.-M. *Electroanalysis* **2011**, *23*, 196−200.
(231) Zhou, Y.; Chen, C.; Baker, L. A. *Anal. Chem.* **2012**, *84*, 3003−3009.
(232) Chen, C.; Zhou, Y.; Baker, L. A. *ACS Nano* **2011**, *5*, 8404−8411.
(233) Sa, N.; Baker, L. A. *J. Am. Chem. Soc.* **2011**, *133*, 10398−10401.
(234) Chen, C.; Derylo, M.; Baker, L. A. *Anal. Chem.* **2009**, *81*, 4742−4751.
(235) Chen, C.; Zhou, Y.; Baker, L. A. *Annu. Rev. Anal. Chem.* **2012**, *5*, 207−228.
(236) Shen, M.; Ishimatsu, R.; Kim, J.; Amemiya, S. *J. Am. Chem. Soc.* **2012**, *134*, 9856−9859.
(237) Elsamadisi, P.; Wang, Y.; Velmurugan, J.; Mirkin, M. V. *Anal. Chem.* **2010**, *83*, 671−673.
(238) Sun, P.; Laforge, F. O.; Abeyweera, T. P.; Rotenberg, S. A.; Carpino, J.; Mirkin, M. V. *Proc. Natl. Acad. Sci. U.S.A.* **2008**, *105*, 443−448.
(239) Schulte, A.; Nebel, M.; Schuhmann, W. *Annu. Rev. Anal. Chem.* **2010**, *3*, 299−318.
(240) Takahashi, Y.; Shevchuk, A. I.; Novak, P.; Babakinejad, B.; Macpherson, J. V.; Unwin, P. R.; Shiku, H.; Gorelik, J.; Klenerman, D.; Korchev, Y.; Matsue, T. *Proc. Natl. Acad. Sci. U.S.A.* **2012**, *109*, 11540−11545.
(241) Morris, C. A.; Chen, C.; Baker, L. A. *Analyst* **2012**, *137*, 2933−2938.